Int. J. Nano Dimens., 9 (4): 386-397, Autumn 2018

ORIGINAL ARTICLE

Influence of synthesis parameters on the properties of nanostructured γ-Alumina using Plackett-Burman experimental design

*Mehrnoosh Kiani [1], Mohammad Yousefi [1, *], Mehdi Rashidzadeh [2], Akbar Irandoukht [2], Fathollah Salehirad [2]*

[1] *Department of Chemistry, Science and Research Branch, Islamic Azad University, Tehran, Iran*
[2] *Catalysis Research Center, Research Institute of Petroleum Industry, Tehran, Iran*

Received 06 April 2018; revised 24 June 2018; accepted 26 June 2018; available online 27 June 2018

Abstract

Mesoporous nanostructured γ-Al_2O_3 powders were synthesized through multi- step precipitation procedures using the pH-swing technique. Structural and morphological characteristics in addition to the thermal behavior of the procured samples were characterized via X-ray diffraction (XRD), field emission scanning electron microscopy (FESEM), fourier transform infrared (FT-IR) spectroscopy, thermogravimetry-derivative thermal gravimetric (TG-DTG) and N_2 adsorption–desorption isotherm. Plackett-Burman design was implemented as a screening method to examine the impacts of fifteen variables on physical properties of synthesized γ-Al_2O_3 as a response variable. Specific surface area, pore volume and average pore diameter of the prepared samples were found to be within the ranges of 72-335.7 m^2/g, 0.26-1.03 cm^2/g and 4.6-15.2 nm, respectively. It was determined that the variables including pH value on the acidic region, time in the alkaline region and number of pH-swing frequencies had major effects on the pore diameter of the procured γ-Al_2O_3 powders. Calcination by steaming had the most significant effect on specific surface area, while the pH value on the acidic region had the greatest impact on pore volume.

Keywords: *Mesoporous; Multi-Step Precipitation; Nanostructure; pH-Swing; Plackett-Burman.*

How to cite this article

Kiani M, Yousefi M, Rashidzadeh M, Irandoukht A, Salehirad F. Influence of synthesis parameters on the properties of nanostructured γ-Alumina using Plackett-Burman experimental design. Int. J. Nano Dimens., 2018; 9 (4): 386-397.

INTRODUCTION

γ-Al_2O_3 is among the most vital inorganic materials utilized in many industries, such as ceramics and catalyst support, due to its high application and physical properties. Within the last decade, the structure of the porous γ-Al_2O_3 has proved valuable to maybe researchers.

One of the most common applications of γ-Al_2O_3 is as a catalyst support. Physical properties and other characteristics of the catalyst support, such as pH, temperature, aging time, raw materials and preparation technique, have a major impact on the performance of the catalyst in hydrotreating processes [1-3].

Thus far, a variety of procedures have been implemented for the synthesis of γ-Al_2O_3, including sol-gel [4, 5], plasma arc [6], and hydrothermal [7]. Sadjadi *et al.* [8] produced alumina nanopowder by combustion method as a catalyst for the synthesis of imidazo[1,2-a]azine. The primary drawbacks of such techniques for synthesis of γ-Al_2O_3 are higher required temperature in plasma arc, lower sol-gel efficiency, extended reaction time in hydrothermal and pollution due to carbon residue in combustion method. In order to bypass these obstacles, a multi-step precipitation process involving a pH-swing technique can be applied. Ono *et al.* [9] was the first to report this procedure and they managed to study the effectiveness of the pH and number of pH-swing frequencies on γ-Al_2O_3 formation. Increases in the number of pH swings resulted in increased pore diameter. Maity

* Corresponding Author Email: myousefi50@hotmail.com

et al. [10] prepared the catalyst supported by alumina via various techniques, such as pH-swing, and determined that this method improved the pore size distribution (PSD). Fernandez *et al.* [11] synthesized SiO_2-Al_2O_3 catalyst support using pH-swing method in a hydrodesulfurization process with specific surface area of about 280-390 m^2/g and obtained an average pore diameter about of 10 nm.

Advantages of pH-swing method include lower preparation time in contrast to traditional methods and greater mechanical strength of synthesized materials. It is appropriate for preparing the alumina support, because it can alter the structure of these materials in different porosity ranges [10]. This technique is suitable for improving the narrow pore size distribution.

Statistical experimental design methodology enhances the product. In this design, the choice of the appropriate algorithm is determined by the objective of the experiment. If the purpose of the experiments is to screen factors or to examine their effects on the response, the Plackett-Burman (PB) design is suited to a minimum number of factor levels. This is one of the most effective methods for screening a vast array of critical parameters and is used to study (K) factor in two levels: High (+) and low (-) [12, 13]. In PB design, if the number of factors is (K), then the number of experiments (N) is obtained from the equation (N = K-1). Researchers have analyzed the effect of different variables such as pH, reaction temperature, etc. on the preparation of γ-Al_2O_3 by classical approaches [9, 14]. But thus far, very little studies have been undertaken to investigate the effect of pH swings with other variables simultaneously.

In this study, we prepared γ-Al_2O_3 samples through a multi-step precipitation method using pH-swing technique. The goal was to investigate the effect of a number variables such as type of acidic precursor, type of alkaline precursor, acid solution concentration, base solution concentration, number of pH-swing frequencies, time in the acidic region, time in the alkaline region, pH value on the acidic region, pH value on the alkaline region, reaction temperature, template (P123), aging time, calcination temperature, calcination time and calcination by steaming on physical properties of the γ-Al_2O_3, such as specific surface area, pore volume, and average pore diameter as a response, using a Plackett-Burman design. Finally, significant variables were found to improve the proper conditions for the preparation of γ-Al_2O_3 as a catalyst support in hydrotreating processes.

EXPERIMENTAL

Characterization

X-ray diffraction (XRD) was applied to determine the crystalline structure of the powders. It was performed using CuKα radiation (λ= 1.54056 Å) on a Philips diffractometer (1840). Pore structure of samples was determined by adsorption apparatus (Micrometrics, ASAP). Total surface area of the samples was measured by Brunauer-Emmett-Teller (BET) method. Pore size distribution and average pore diameter were determined from the desorption branch of the isotherm using Burrett-Joyner-Halenda (BJH) method (Model Tri-Star II 3020). Fourier transform infrared (FT-IR) spectra of the samples were done using a spectrometer (Model Vertex 70, Bruker) in the wavelength range 400-4000 cm^{-1}. Field emission scanning electron microscopy (FESEM, Model Mira3 Tescan) was used to study surface morphology and particle size. TG-DTG analysis was undertaken by a TGA1 Mettler Toledo instrument under a stream of dry N_2 flowing with a heating rate 10 $^oC\ min^{-1}$.

Materials and methods

Aluminum nitrate ($Al(NO_3)_3.9H_2O$), aluminum sulfate ($Al_2(SO_4)_3.18H_2O$), ammonia (NH_3 25wt %), nitric acid (HNO_3 65wt %), sulfuric acid (H_2SO_4 97wt %), are all laboratory-grade were purchased from Merck company. Sodium aluminate ($NaAlO_2$), Pluronic P123 (PEO-PPO-PEO triblock copolymer), M_{av}=5800 as a template were purchased from Sigma- Aldrich, and ammonium carbonate $(NH_4)_2CO_3$ was purchased from Chem.lab. Fifteen variables were selected with two coded levels (Table 1). A plackett-Burman matrix with sixteen trials designed as shown in Table 2.

Samples were prepared in accordance with Table 2. In order to prepare sample R1, for example, the first pH-swing operation was started by adding a certain amount of $Al(NO_3)_3.9H_2O$ into a glass reactor and terminated with the addition of sodium aluminate solution. Solution pH ranged between 4 and 10, and reaction time was 5 and 2 minutes in acidic and alkaline regions, respectively. The resulting gel was kept at 50 ^oC for 20 h. Then, obtained gel were filtered and rinsed with a hot water. After filtration, the sample was dried at 120 ^oC for 4 h, and then calcined in a stove with a heating rate of 2 $^oC\ min^{-1}$ at 500 ^oC for 3h.

Table 1. Variables and their levels for preparation of samples.

Variables	Units	Symbol	Low level	High level
Type of acidic precursor	-	AR	aluminum sulfate	Aluminum nitrate
Type of alkaline precursor	-	BR	ammonium carbonate	Sodium aluminate
Concentration of acid solution	M	AC	0.5	0.7
Concentration of base solution	M	BC	1.5	2.1
Number of pH swing frequencies	-	F	3	6
Time in the acidic region	min	AT	2	5
Time in the alkaline region	min	BT	2	5
pH value on the acidic region	-	ApH	2	4
pH value on the acidic region	-	BpH	8	10
Reaction temperature	˚C	TR	50	80
Template (P123)	-	TT	No	Yes
Aging time	h	T-age	1	20
Calcinations temperature	(˚C)	T-cal	500	600
calcination time	h	Time	3	5
Calcination by steaming	-	TST	No	Yes

Table 2. Plackett- Burman design matrix with sixteen trials.

Run \ Variable	AR	BR	AC	BC	F	AT	BT	ApH	BpH	TR	TT	T-age	T-cal	Time	TST
R1	+	+	+	+	-	+	-	+	+	-	-	+	-	-	-
R2	-	+	+	+	+	-	+	-	+	+	-	-	+	-	-
R3	-	-	+	+	+	+	-	+	-	+	+	-	-	+	-
R4	-	-	-	+	+	+	+	-	+	-	+	+	-	-	+
R5	+	-	-	-	+	+	+	+	-	+	-	+	+	-	-
R6	-	+	-	-	-	+	+	+	+	-	+	-	+	+	-
R7	-	-	+	-	-	-	+	+	+	+	-	+	-	+	+
R8	+	-	-	+	-	-	-	+	+	+	+	-	+	-	+
R9	+	+	-	-	+	-	-	-	+	+	+	+	-	+	-
R10	-	+	+	-	-	+	-	-	-	+	+	+	+	-	+
R11	+	-	+	+	-	-	+	-	-	-	+	+	+	+	-
R12	-	+	-	+	+	-	-	+	-	-	-	+	+	+	+
R13	+	-	+	-	+	+	-	-	+	-	-	-	+	+	+
R14	+	+	-	+	-	+	+	-	-	+	-	-	-	+	+
R15	+	+	+	-	+	-	+	+	-	-	+	-	-	-	+
R16	-	-	-	-	-	-	-	-	-	-	-	-	-	-	-

Steaming was also carried out in a tubular furnace where the water injection rate was at 0.3mL min^{-1} in the relevant experiments. In the samples that used P123, the amount used was 1.0 g and the pH of the solutions on the acidic and alkaline regions were adjusted by using sulfuric acid, nitric acid solution and aqueous NH_4OH.

RESULT AND DISCUSSION

Crystalline structure

During the preparation [15, 16], the chemical reactions (reactions 1-5) that occurred are highlighted as changes in the various crystalline phases observed in the XRD pattern and indicate that variables of solution pH and kind of precursors are important in the formation of the products. It can therefore be said that sodium aluminate and ammonium carbonate utilized in these samples as precipitant agents lead to the formation precursors of Pseudoboehmite (PB) and ammonium aluminum carbonate hydroxide (AACH), respectively.

$$Al_2(SO_4)_3 + 6\,NaAlO_2 + 12H_2O \longrightarrow 8Al(OH)_3 + 3\,Na_2SO_4 \quad (1)$$

$$Al(OH)_3 \longrightarrow AlOOH + H_2O \quad (2)$$

$$Al_2(SO_4)_3 + 3(NH_4)_2CO_3 + 3\,H_2O \longrightarrow 2\,Al(OH)_3 + 3(NH_4)_2SO_4 + 3CO \quad (3)$$

$$(NH_4)_2CO_3 + H_2O \rightleftharpoons 2NH_4^+ + HCO_3^- + OH^- \quad (4)$$

$$AlOOH + HCO_3^- + NH_4^+ \longrightarrow NH_4AlO(OH)HCO_3 \quad (5)$$

The XRD analysis was performed for all samples. For instance, the XRD pattern of samples R2 and R7 are compared based upon the type of alkaline precursor. Fig. 1 shows the XRD pattern of the dried samples R2 and R7. As shown in Fig. (1a), PB phase with orthorhombic structure (JCPDS-No. 83-2384) was formed in sample R2 (reactions 1, 2). Intensity of weak and broad peaks indicates that the particle size of the procured sample is small. As shown in Fig. (1b), for sample R7, AACH phase with a chemical composition of $NH_4AlO(OH)HCO_3$ was formed (JCPDS No. 42-0250) (reactions 3-5). The high intensity of the peaks reveals that the AACH phase is highly crystalline. In both samples, the reactants are mixed in deionized water and allowed in the pH=10 at 80 °C.

Fig. 2 shows XRD patterns of γ-Al_2O_3 phase of samples R2 and R7. All diffraction peaks of the samples display cubic symmetry and are highly consistent with standard diffraction data (JCPDS: 00-029-0063). These broad diffraction peaks indicate that the structure of the produced samples is nano-sized. The most important peaks in the XRD pattern correspond to 2θ of 39.5, 45.8 and 66.8, which are related to (222), (400) and (440) reflections (Fig. 2a) [16], respectively. Using the Scherrer equation $D= 0.9\lambda/\beta\cos\theta$, crystal size of calcined sample R2 was 4.4 nm. In Fig. (2b) poorly crystallized γ-alumina can be seen which may be a consequence of the decomposition of

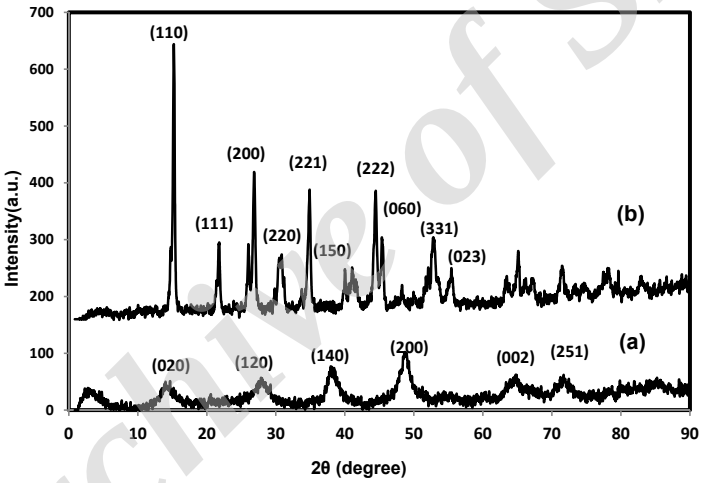

Fig. 1. XRD pattern of the dried samples a) R2 and b) R7.

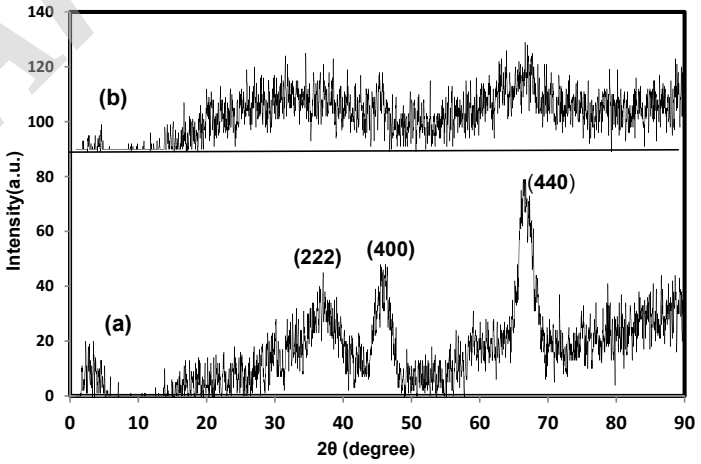

Fig. 2. XRD pattern of the γ-Al_2O_3 samples a) R2 and b) R7.

AACH and the release of CO_2, NH_3, and H_2O.

Alternatively, AACH prepared from aluminum sulfate precursor during calcination at 300 to 700 °C, is transformed to amorphous alumina and γ-Al_2O_3 begins to appear at 800 °C, which was verified by previous studies [17, 18].

Pore structure

Fig. 3 displays the N_2 adsorption-desorption isotherms of γ-Al_2O_3 samples. In every sample, except R4 and R8 (Fig. 3a); the type IV isotherm is present, indicating that the samples are in the mesoporous nature with hysteresis loops of the H2 and H3 type. In a few curves such as (R3, R8, R12, R13,...), hysteresis loop shifted to the region with greater relative pressure, implying that the pore volume decreased, resulting in a larger pore size and broader pore size distribution, which is clearly demonstrated in the patterns of the PSD curves (Fig. 4). Isotherm of samples R4 and R8 procured from AACH are type VI (stepwise), which are related to the absorption of the layer by layer on an entirely uniform surface [19]. There are two hysteresis loops in their isotherm that correspond to the double pores distribution (Fig. 3a and Fig. 4a, b). It therefore seems that some of the γ-Al_2O_3 samples prepared from PB are approximately narrow pore size distribution, while most samples obtained from AACH have two pore size distributions (Fig. 4). The smaller pores demonstrate narrow PSD curves and larger pores exhibit more expansive PSD curves. These differences arise from the formation of distinctive pore mechanisms. In samples R9, R10, R13, and R16, with low pH value on the acidic region and low the time in alkaline region, the pore size distribution shifted to the larger pore size region. Consequently, it is suggested that the porous structure of alumina is reliant on the reduction or increase in pH value on the acidic region, the number of pH-swing frequencies, the time in alkaline region and different kind of precursor. Scientists have already noted the significance of these variables in structural and texture properties of γ-alumina.

TG-DTG analysis

The thermal behavior of dried samples R2 and R7 by TG-DTG analysis is highlighted in Fig. 5. As displayed, the variation between these two samples is a result of the presence of two species of HCO_3^- and OH^- in the formed alumina precipitates. In Fig.(5a), the TG curve reveals three-stage weight loss that can be used to explain the thermal transformation of pseudoboehmite into γ-alumina: (1) At temperatures under 100 °C, about 9.61% a decrease in weight is associated with the evaporation of adsorbed water molecules that exist in pseudoboehmite pores. (2) From 150 to 500 °C, a loss in weight is about 18.03% attributed to the dehydroxylation process and crystallization of transition γ-Al_2O_3. (3) When

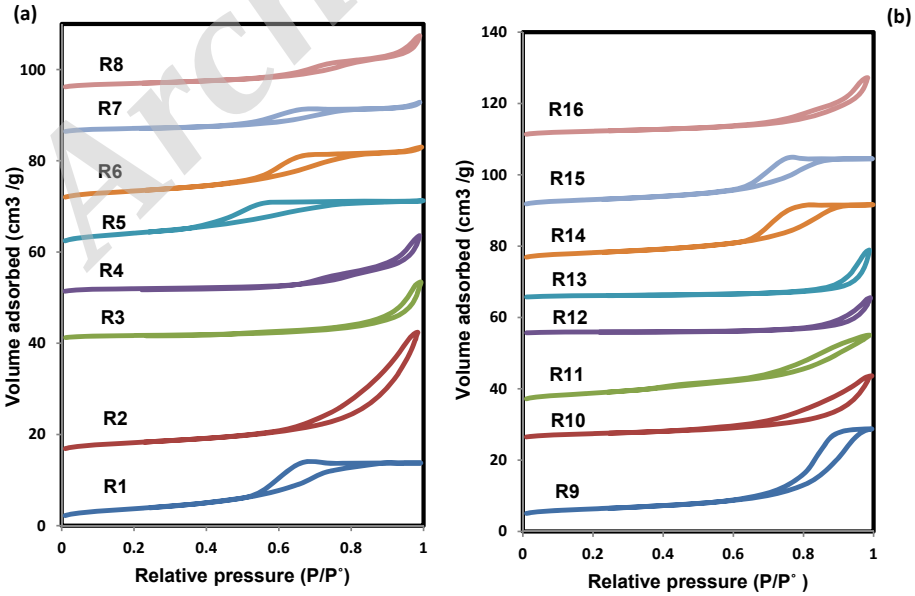

Fig. 3. Nitrogen adsorption-desorption isotherms for calcined samples a) R1-R8 and b) R9-R16.

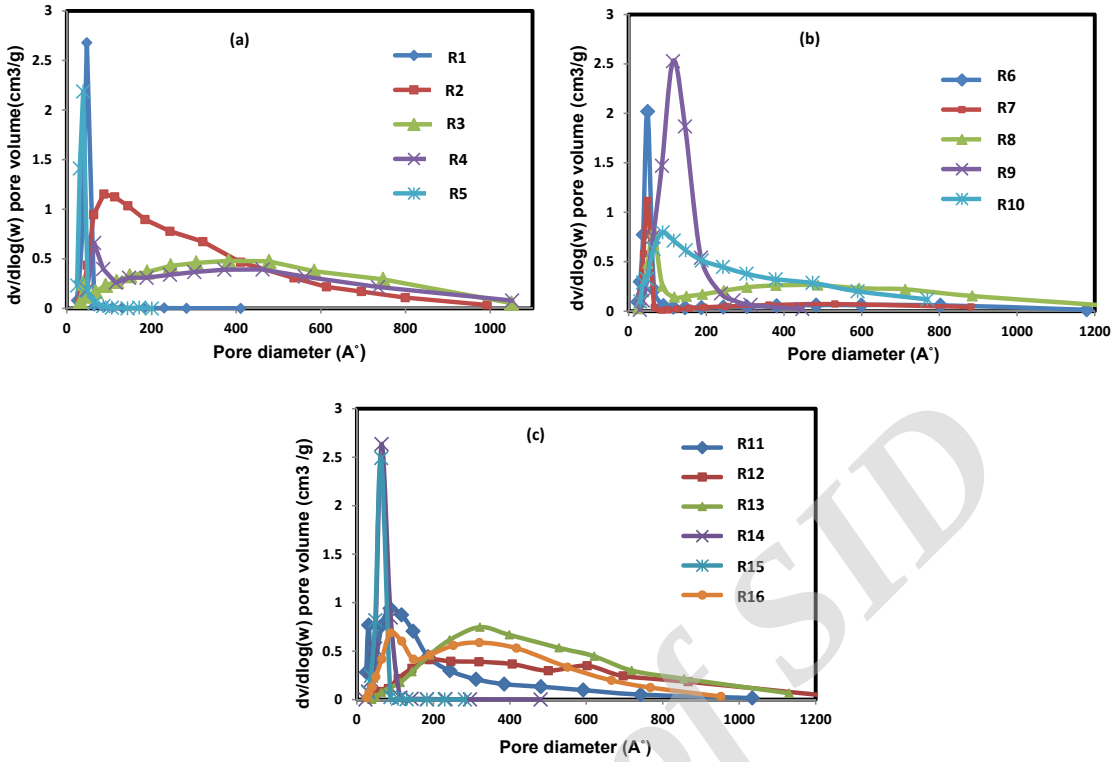

Fig. 4. PSD curves of calcined samples: a) R1-R5, b) R6-R10 and c) R11-R16.

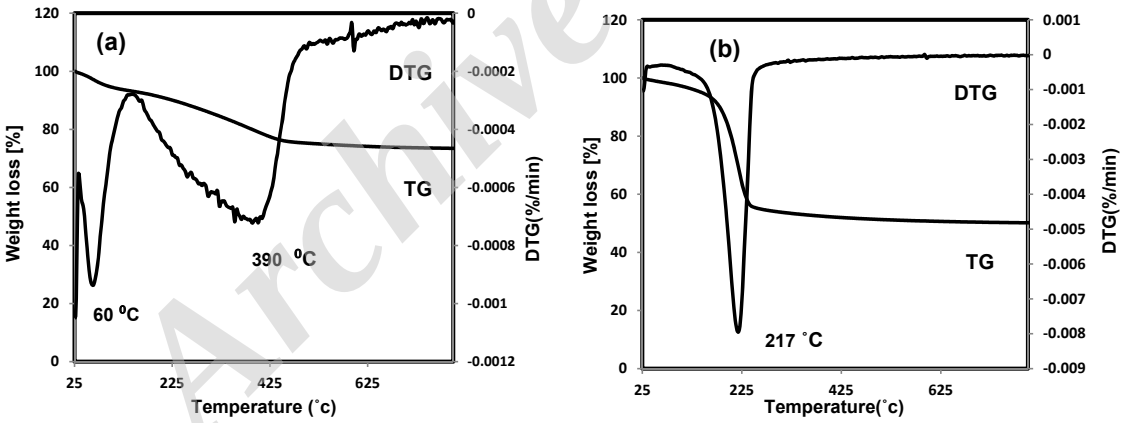

Fig. 5. TG-DTG curves for dried samples a) R2 and b) R7.

the temperature increased from 500 to 800 °C, the weight loss of 1.6% is related to the removal of the remaining hydroxyls in the crystalline structure of γ-alumina. In the DTG curve the minor exothermic peak around 60 °C and a broad exothermic peak at 390 °C can be attributed to the removal of adsorbed water and the weight loss of phase transformation from γ-AlOOH to γ-Al_2O_3, respectively. The thermal behavior of sample R2 is therefore in accordance with what observed in the results published previously [20]. The TG curve of the sample R7 shows a slight weight loss below 150 °C is associated with desorption of the physically adsorbed water (Fig. 5b). The second decrease in weight in the temperature range of 127 to 280 °C is a result of the decomposition of AACH, which releases CO_2, NH_3, and H_2O and forms AlOOH particles. The gradual weight loss above 300 °C is maybe attributed to the decomposition of AlOOH and the phase transition of γ-Al_2O_3. In

addition, it is mentioned that the DTG curve of sample R7, a major exothermic peak at around 217 °C, which could be due to the decomposition of AACH. Theoretically, in the TG-DTG analysis, the transformation of the phase of γ-AlOOH and AACH to γ-Al_2O_3 occurs according to the decomposition reactions 1-5 mentioned previously which is comparable to the literature [16, 21].

FTIR measurement

The FTIR spectra of samples R2 and R7 is shown in Fig. 6. In both samples, there is broad absorption bands at 3300-3500 cm^{-1} associated with O-H stretching of adsorbed water. Fig. (6a) shows the peaks associated with the pseudoboehmite phase. Band at 1640 cm^{-1} belongs to bending vibration of H-OH in H_2O molecules. Adsorption peak around 1385 cm^{-1} corresponds to deformation vibrations of H_2O. The sharp peak at 1070 cm^{-1} is related to symmetrical Al-OH bending modes. In Fig. (6b), bands at 751,856, 1106, 1450 and 1545 cm^{-1} are attributed to CO_3^{-2} anions in the AACH structure. Obvious bands at 1390, 1721, 1830, 3029, 3102 and 3174 cm^{-1} are related to NH_4^+ groups. The sharp band at 981 cm^{-1} is assigned to Al-OH vibration. In Fig. 6c, d, FTIR spectra of γ-Al_2O_3 in samples R2 and R7 are displayed. The adsorption peak at 1635 cm^{-1} belongs to bending vibration of O-H group in the adsorbed water. The bands at 500-750 cm^{-1} correspond to Al-O vibrations in the γ-Al_2O_3 structure, in particular stretching and bending vibrations of AlO_6. Absorption bands in the presented spectra are in accordance with the IR spectra of γ-AlOOH, AACH and γ-Al_2O_3 reported in previous studies [15, 21].

FESEM analysis

The FESEM images of γ-Al_2O_3 samples R2 and R7 reveal that the particles are nano-sized. Synthesized samples demonstrate strong agglomeration of spherical particles and have large porosity. (Fig. 7).

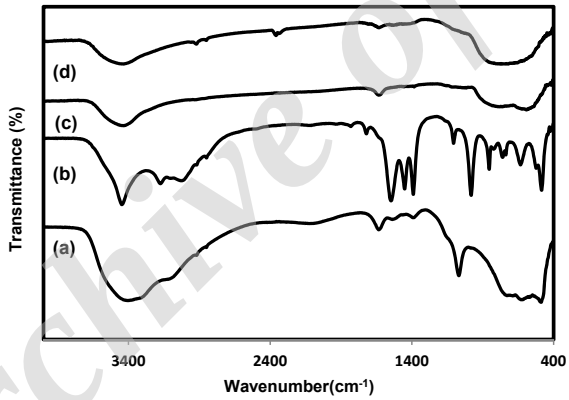

Fig. 6. FTIR spectrum of the dried sample of a): R2, b): R7 and calcined samples c): R2, (d): R7.

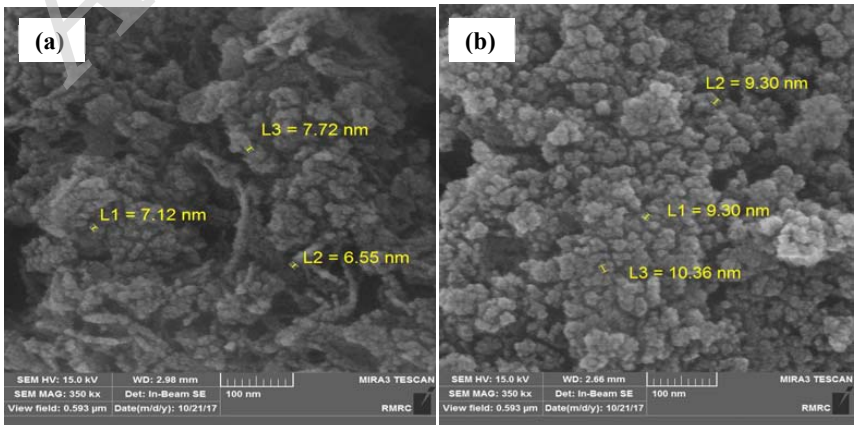

Fig.7. FESEM images of calcined samples: a) R2 and b) R7.

Results of Plackett- Burman Analysis

Plackett- Burman design determines the significant variables affecting on selected responses. These analyzed responses are characteristics of specific surface area, pore volume and average pore diameter. The experimental results are presented in the Table 3. E_x represents the effects of each variable on the responses are shown in Table 4. The following equation formulates the impact of each of the variables on the desired response.

$$EX = \frac{\sum Y(+) - \sum Y(-)}{N/2} \quad (1)$$

Where ∑Y refers to the sum of the selected responses at the high and low levels of each variable (x) and N is the total number of trials. The negative and positive signs of the variables obtained from equation (1) mean that changes in variables from low to high level have a negative and positive effect on the response, respectively.

To determine variables that have significant effects and in order to estimate the error standard deviation, the half normal probability plot is used as a graphical interpretation approach of Plackett-Burman design on the responses [22] (Fig. 8). Points that deviate far from the straight line passing through the other points indicate that

Table 3. Experimental results of Physical properties of the different γ-Al_2O_3 samples.

Samples	Surface area (m^2/g), Y1	Pore volume (cm^3/g), Y2	Average pore diameter (nm), Y3
R1	283	0.41	5.9
R2	272	1.03	15.2
R3	130.1	0.38	11.8
R4	150.6	0.42	11.1
R5	335.7	0.39	4.6
R6	272.5	0.43	6.4
R7	163.9	0.26	6.3
R8	157	0.39	10
R9	267	0.89	13.3
R10	196.1	0.6	12.3
R11	308.8	0.68	8.8
R12	72.3	0.3	17.0
R13	91.3	0.39	17.3
R14	257.7	0.57	9
R15	248	0.51	8.2
R16	181.6	0.53	11.8

Table 4. Numerical value of the effects of variables on responses.

Variables	Specific surface area (m^2/g)	Pore volume (cm^3/g)	Average pore diameter (nm)
AR	63.76	0.03	-2.07
BR	43.73	0.16	0.46
AC	-0.23	0.04	0.10
BC	-15.63	0.02	1.28
F	-31.64	0.05	3.31
AT	5.73	-0.12	-1.32
BT	78.78	0.05	-3.92
ApH	-7.88	-0.25	-3.78
BpH	-9.07	0.03	0.46
TR	21.49	0.1	-0.3
TT	9.19	0.05	-0.86
T-age	20.95	-0.035	-1.02
T-cal	2.94	0.03	1.99
Time	-32.51	-0.04	1.58
TST	-89.25	-0.16	1.45

they are the variables that have significant effects, whereas the other points have negligible effects. Based on Table 4 and Fig. (8a), significant variables for the specific surface area are calcination by steaming (TST), time in the alkaline region (BT), the type of acid and alkaline precursors (AR and BR), calcination time (Time) and the number of pH-swing frequencies (F), respectively. Fig. (8b) displays the half normal probability plot for pore volume, which verifies that variables including the pH value on the acidic region (ApH), calcination by steaming (TST), the type of alkaline precursor (BR), time in the acidic region (AT) and reaction temperature (TR) have notable effects on pore volume, respectively. As shown in the Fig. (8c), variables that significantly impact on average pore diameter are time in the alkaline region (BT), pH value on the acidic region (ApH) and the number of pH-swing frequencies (F), respectively.

Fig. 9 provides the main effect plots of the selected variables that have the greatest effect on specific surface area and they illustrate the impact of each of the variables at its lowest and highest levels and examine the average changes that occur in the responses. The slope of each plot shows the effect of the relevant variable on the desired response. As shown in Fig. 9(a,b), Increasing the time in the alkaline region causes increases

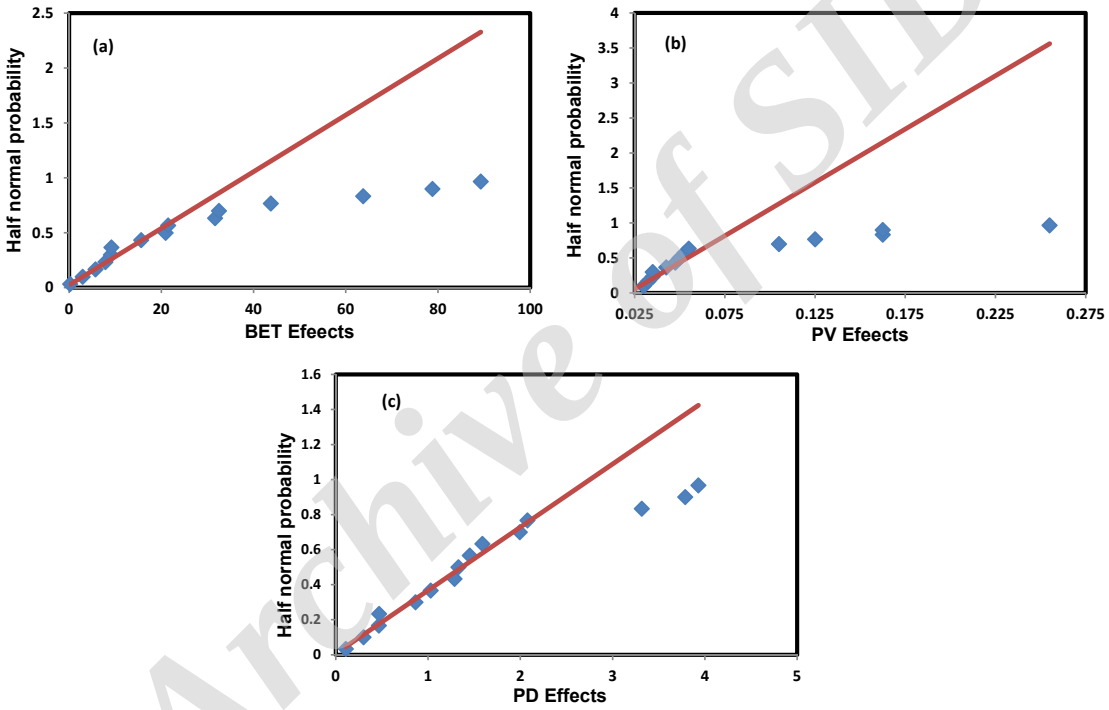

Fig. 8. Half normal probability plots of the variables affecting on a) specific surface area b) pore volume c) average pore diameter.

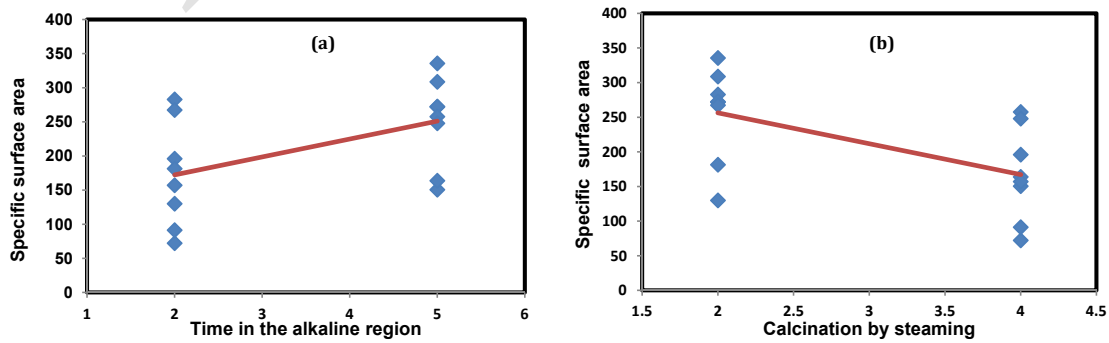

Fig. 9. Main effect plots for two most significant variables: a) Time in the alkaline region and b) Calcination by steaming on specific surface area.

in specific surface area, but the utilization of steaming decreases the surface area, respectively. On the other hand, increasing pH value on the acidic region (ApH) and applying steaming have negative effects on pore volume, (Fig. 10 a,b). Physical properties that control γ-Al_2O_3 performance could possibly have reverse trends. As it is known, when the special surface area rises, the pore diameter is reduced. The thermal and hydrothermal (calcination by steaming) conditions and characteristics of γ-AlOOH and AACH precursors cause changes in the properties of alumina which are very important. In the present work, one of the important variables in the preparation of γ-Al_2O_3 powder is the effect of calcination by steaming on the physical properties of γ-Al_2O_3. γ-alumina is produced with larger crystallites when its precursors are subjected to calcination by steaming. Arguably, water molecules assist in transporting aluminum atoms to grow crystals, which causes small crystalline aggregates absent from these samples [23], and

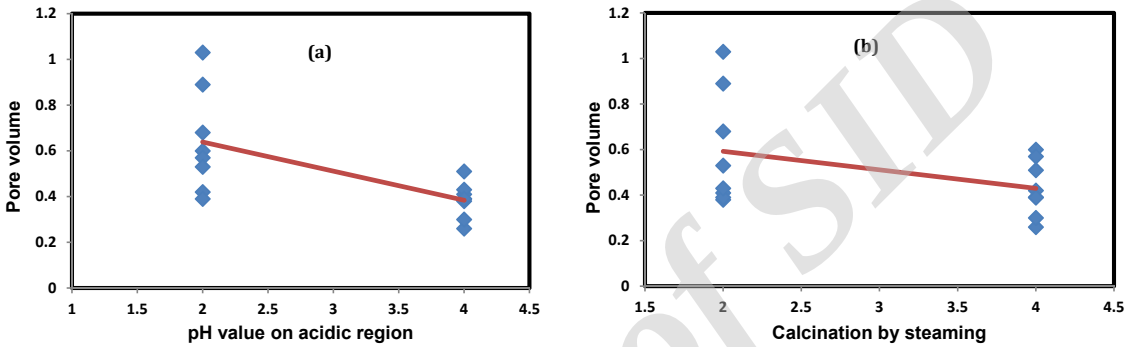

Fig. 10. Main effect plots for two most significant variables: a) pH value on acidic region and b) Calcination by steaming on pore volume.

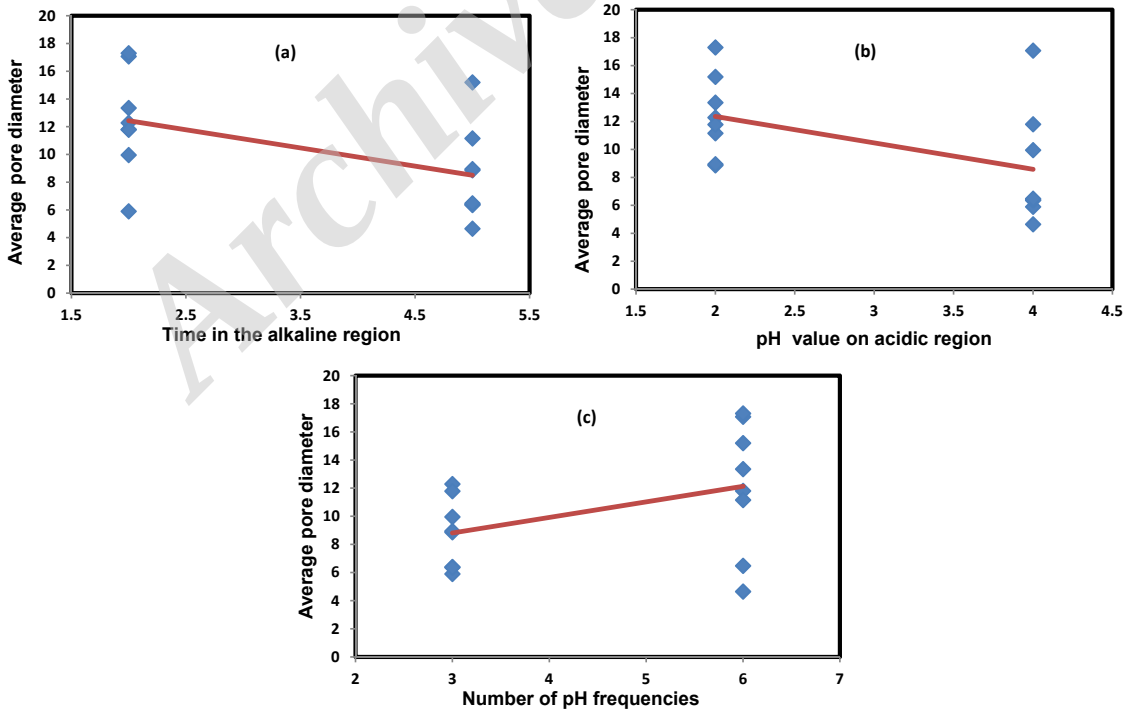

Fig. 11. Main effect plots for three most significant variables: a) Time in the alkaline region, b) pH value on acidic region and c) Number of pH freqencies on verage pore diameter.

it can therefore be concluded that calcination in steaming conditions inhibits the production of small crystalline agglomerates and results in the formation of γ-Al_2O_3 with larger crystallites; ultimately reducing specific surface area and pore volume, and increasing pore size distribution [24].

As seen in the Fig. 11, the increase in time in alkaline region (BT), pH value on the acidic region (ApH) and the number of pH-swing frequencies have negative (Fig. 11 a,b) and positive correlations on the average pore diameter (Fig. 11c). It was confirmed that when pH=2 in the multi-step precipitation method, the amorphous aluminum hydroxide formed in the reaction is well dissolved and relatively uniform dried precursors consists of PB and AACH are obtained. Clearly, the number of pH-swing frequencies is a vital parameter in the multi-step precipitation method for controlling the pore diameter of γ-Al_2O_3. Alternative frequencies caused fine particles like amorphous aluminum hydroxide to be dissolved in acidic regions. In the alkaline region, the dissolved aluminum hydroxide then precipitates on the dried precursors and assists in their growth. After several repetitions of pH-swing, it may eventually be possible to obtain more uniform γ-alumina precursors and γ-alumina particles with relatively narrow pore distribution. In order to synthesize γ-Al_2O_3, it is necessary to have an appropriate pH value and sufficient reaction time. The production of pseudoboehmite only needs a short reaction time in the alkaline and acidic region. Preparation of γ-Al_2O_3 at a shorter reaction time results in the hydrosol particles formed during the reaction to be uniformly sized. If the hydrosol is long maintained in the acidic or alkaline region, crystal growth becomes more challenging and these outcomes are consistent with the research conducted by Ono *et al.* [9, 25].

CONCLUSION

To synthesize nanostructured γ-alumina, a multi-step precipitation method with pH-swing technique was implemented. The XRD patterns indicated that the prepared γ-Al_2O_3 had low crystallinity and FESEM images showed that particles size is nanometer scale. The PB design was utilized to evaluate obtained data and identify the significant factors from a large number of variables. Time in the alkaline region, pH value on the acidic region and calcination by steaming are the most important of the factors as they have major impact on the physical properties of the γ-Al_2O_3. The main information from this design can be the ultimate goal for future studies that can be fixed or altered to optimize responses at more levels.

ACKNOWLEDGMENTS

The authors are grateful to the Research Institute of Petroleum Industry and Department of Chemistry, Science and Research Branch, Islamic Azad University for their financial support of the authors of this article.

CONFLICT OF INTEREST

The authors declare that there are no conflicts of interest regarding the publication of this manuscript.

REFERENCES

[1] Maryani E., Abdullah, M., Dayamanti H., Septawendar R., (2016), Effect of ultrasonic irradiation on the characteristic of γ-Al_2O_3 nanorods synthesized from nitrate salt-starch precursors trough a facile precipitation method. *J. Ceram. Soc. Japan*. 124: 1205-1210.

[2] Amirsalari A., Farjami S., (2015), Effect of pH and calcinations temperature on structural and optical properties of alumina nanoparticles. *J. Superlatt. Microstruct.*82: 507-524.

[3] Da-Ros S., Barbosa-Coutinho E., Schwaab M., Calsavara V., Fernandes-Machado N. R. C., (2013), Modeling the effects of calcination conditions on the physical and chemical properties of transition Alumina catalysts. *J. Mater. Character.* 80: 50-61.

[4] Alves A. K., Berutti F. A., Bergmann C. P., (2005), The effects of pH on the preparation of alumina by Sol-Gel process. *J. Particul. Sci. Technol.* 23: 351-360.

[5] Ellateif T. M., Maitra S., (2017), Some studies on the surface modification of sol-gel derived hydrophilic Silica nanoparticles. *Int. J. Nano Dimens*. 2: 97-106.

[6] Madhu K. P., Balasubrarnanian C., Sali N. D., (1999), Nanophase alumina synthesis in thermal arc plasma and characterization: correlation to gas-phase studies. *J. Mater. Sci. Eng. B. Solid*. 63: 215-221.

[7] Qu L., He C., Yang Y., He Y., Liu Z., (2005), Hydrothermal synthesis of alumina nanotubes templated by anionic surfactant. *J. Mater. Lett.* 59: 4034-4037.

[8] Sadjadi S., Rasouli S., (2011), An efficient synthesis of imidazo [1,2-a] azine using nanocrystalline Alumina powder. *Int. J. Nano. Dimens.* 3: 177-186.

[9] Ono T., Ohguchi Y., Togari O., (1983), Control of the pore structure of porous alumina. *J. Prep. Catalysts III*. 1: 631-641.

[10] Maity S. K., Ancheyta J., Rana M. S., (2005), Support effects on hydroprocessing of maya heavy crude. *J. Energy and Fuel*. 19: 343-347.

[11] Fernandez. V. C., Ramrez J., Alejandre A. G., Sanchez-

Minero F., Cuevas-Garcıa R., Torres-Mancera P., (2008), Synthesis, characterization and evaluation of $NiMo/SiO_2$–Al_2O_3 catalysts prepared by the pH-swing method. *J. Catal. Today*. 130: 337–344.

[12] Plackett R. L., Burman J. P., (1964), The design of optimum multifactorial experiments. Biometrika. 33: 305–325.

[13] Farrokhnia M., Safekordi A., Rashidzadeh M., Khanbabaei G., Akbari Anari R., Rahimpour M., (2016), Development of porous nanocomposite membranes for gas separation by identifying the effective fabrication parameters with Plackett–Burman experimental design. *J. Porous Mater*. 23: 1279–1295.

[14] Lopez J. A., Toledo J. A., Escobar J., Salinas E., (2008), Preparation of Alumina–Titania nanofibers by a pH-swing method. *J. Catal. Today*. 133–135: 113–119.

[15] Liu Ch., Li J., Liew k., Zhu J., Bin Nordin M. R., (2012), An environmentally friendly method for the synthesis of nano-alumina with controllable morphologies. *J. RSC Adv*. 2: 8352–8358.

[16] Wuy Y. S., Ma J., Hu F., Li M. C., (2012), Synthesis and characterization of mesoporous Alumina *via* a reverse precipitation method. *J. Mater. Sci. Technol*. 28: 572-576.

[17] Sun X., Li J., Zhang F., Qin X., Xiu Zh., Ru H., (2003), Synthesis of nanocrystalline γ-Al_2O_3 powders from nanometric ammonium aluminum carbonate hydroxide. *J. Am. Ceram. Soc.* 86: 1321-1325.

[18] Xiuhong M., Linhai D., Xiaohua X., Qiang W., Haiyan W., (2014), Synthesis of macro mesostructured γ-Al_2O_3 with large pore volume and high surface area by a facile secondary reforming method. *J. China Petrol. Process. Petrochem. Technol.* 16: 20-28.

[19] Wu Y. S., Ma J., Li M. C., Hu F., (2013), Synthesis of γ-Al_2O_3 with high surface area and large pore volume by reverse precipitation-azeotropic distillation method. *J. Chem. Res. Chinese Univ.* 29: 1-4.

[20] Xu N., Liu Zh., Bia Sh., Dong Y., Li W., (2016),Template-free synthesis of mesoporous γ-Alumina with tunable structural properties. *J. Ceram. Int.* 42: 4072–4079.

[21] Zhu Zh., Sun H., Liu H., Yang D., (2010), PEG-direct hydrothermal synthesis of alumina nanorods with mesoporous structure via AACH nanorod precursors. *J. Mater. Sci*. 45: 46-54.

[22] Daniel C., (1959), Use of half-normal plots in interpreting factorial two-level experiments. *Technometrics.* 1: 311–341.

[23] Guzman-Castillo M. L., Bokhimi X., Toledo-Antonio A., Salmones-Blasquez J., Hernandez-Beltran F., (2001), Effect of boehmite crystallite size and steaming on Alumina properties. *J. Phys. Chem.* 105: 2099-2106.

[24] Mamchick A. I., Kalinin S. V., Vertegel A. A., (1998), Cryosol synthesis of nanocrystalline Alumina. J. Chem. Mater. 10: 3548-3554.

[25] Shiroto Y., Ono T., Asaoka S. (1983). Nakamura M. U.S Patent 4422960.